Hence for a cylinder the intensity of any line element of the profile obeys the proportionality

$$I \propto \int_0^c \exp\left[-\mu(p+c-x)\right]\mathrm{d}x\,. \qquad \text{(A.7)}$$

References

BOND, W. L. (1959). *Acta Cryst.* **12**, 375–381.

CLAASEN, A. (1930). *Phil. Mag.* **9**, 57–65.

DWIGGINS, C. W. JR (1974). *Acta Cryst.* A**31**, 146–148.

DWIGGINS, C. W. JR (1975). *Acta Cryst.* A**31**, 395–396.

EVANS, H. T. & EKSTEIN, M. G. (1952). *Acta Cryst.* **5**, 540–542.

International Tables for X-ray Crystallography (1959). Vol. II, pp. 291–305. Birmingham: Kynoch Press.

TAYLOR, A. & SINCLAIR, H. (1945). *Proc. Phys. Soc.* **57**, 108–125.

WEBER, K. (1967). *Acta Cryst.* **23**, 720–725.

WEBER, K. (1969). *Acta Cryst.* B**25**, 1174–1178.

Acta Cryst. (1976). A**32**, 648

Transmitted-Beam Absorption Pattern from a Turbostratic Structure: Pyrolytic Graphite

BY L. D. CALVERT*

Division of Chemistry, National Research Council of Canada, Ottawa, Canada, K1A OR9

AND R. C. G. KILLEAN† AND A. MCL. MATHIESON

Division of Chemical Physics, CSIRO, P.O. Box 160, *Clayton, Victoria, Australia* 3168

(*Received* 16 *January* 1976; *accepted* 29 *January* 1976)

By the use of Cu $K\alpha_1$ plane-polarized X-rays, the intensity of the beam transmitted through a plate of highly oriented pyrolytic graphite is measured as the plate is tilted (ω) relative to the beam. The resultant transmitted-beam absorption pattern(TBAP), expressed as effective attenuation coefficient, μ', *versus* ω, is interpreted in relation to the turbostratic structure of pyrolytic graphite. The TBAP, μ' *versus* ω, is complementary to the diffraction pattern, presented as log I *versus* 2θ. Potential uses of the TBAP are discussed.

Introduction

In studies of the X-ray polarization ratio for 000*l* reflexions from highly oriented pyrolytic graphite (HOPG) (Calvert, Killean & Mathieson, 1974*a*), the intensity of the transmitted X-ray beam was measured. From a selected range of these measurements, the attenuation coefficient, μ, of carbon for Cu $K\alpha_1$ was deduced (Calvert, Killean & Mathieson, 1975). The transmitted-beam measurements, extended to cover the angular range of the specimen, $\omega = 10$ to 95° ($\omega = 90°$ corresponded to the beam normal to the plane of the specimen), and converted to the effective attenuation coefficient, μ', illustrate the scattering process which occurs with a turbostratic specimen. The derived transmitted-beam absorption pattern, μ' *versus* ω, can be considered as complementary to the diffraction pattern, given as log I *versus* 2θ.

Attention is drawn to the implications of these observations for the determination of accurate attenuation coefficients and accurate absolute intensities.

Experimental

The specimen used was a plate of HOPG (Union Carbide Co., grade ZYA), dimensions approximately $1 \times \frac{1}{2} \times \frac{1}{20}''$ ($2{\cdot}5 \times 1{\cdot}25 \times 0{\cdot}11$ cm) with a nominal crystalline angular spread of $\frac{1}{2}°$ (Moore, 1973). The plate could be tilted (Mathieson, 1968) with respect to the incident beam of plane-polarized Cu $K\alpha_1$ X-rays (Calvert, Killean & Mathieson, 1974*b*) of circular cross section and having a divergence of $\pm 7'$ of arc (aperture near effective source, 1·4 mm, aperture near specimen, 1·66 mm, separation 398 mm) and intensity 16000 counts/s (c/s). The dead time of the counting system ($2{\cdot}54 \times 10^{-6}$ s) was measured by the method of Chipman (1969); the background count rate was 0·15 c/s; counting times were chosen to give precisions ranging between 0·15 and 0·5%. The angular range studied was from $\omega = 95$ to 10°. This gave a range of count rates from 6000 c/s to 20 c/s over a sixfold increase of path length through the specimen; the mean thickness of the specimen, 0·1091 cm, was measured by a specially constructed Sheffield air gauge and also with the aid of a sensitive micrometer (*vide* Calvert, Killean & Mathieson, 1975).

The incident X-ray beam was plane polarized in a vertical plane and the specimen tilt axis was also

---

* N.R.C. No. 15309.

† On leave from School of Physical Sciences, University of St. Andrews, North Haugh, St. Andrews, Scotland KY16 9SS.

vertical so that the effective σ polarization factor remained constant at 1·0 over the full range of ω.

Data

The range of measured intensities was of the order of 300:1 so that display of the full range of the experimental data would be inconvenient. However, presentation of a limited portion of the original intensity data is of interest. Thus, when the specimen was oriented to span the region of reflexion of 0002 ($\omega \sim 11$–$16°$), point-by-point measurement of the transmitted beam yielded a profile shown in Fig. 1(*a*).

For the presentation of the full ω range and interpretation of the scattering process, it is more convenient to convert the data to μ', defined as follows. For the tilt angle ω, the transmitted intensity I is related to the incident intensity I_0 by

$$I = I_0 \exp(-\mu' t \operatorname{cosec} \omega), \qquad (1)$$

where μ' is an effective attenuation coefficient and t is the thickness of the specimen. The detailed results for 0002, corresponding to those in Fig. 1(*a*), are shown in Fig. 1(*b*), while the results for the full ω range, 10 to 95°, are presented in Fig. 2(*a*). The base-line value μ (Calvert, Killean & Mathieson, 1975) corresponds to the normal attenuation coefficient for carbon in HOPG. Deviations of μ' from this value occur whenever any additional scattering process takes place over and above that normally considered in deriving the attenuation coefficient. In the present case, the angular divergence of the incident beam is less than that of the crystallites in the specimen so that instrumental broadening is a relatively minor effect. Hence, the occurrence of additional energy abstraction from the incident beam is directly evident in our results and is not smeared out as it was in the first observations of this aspect of X-ray diffraction experimentation (Bragg, 1914). Under these circumstances, the magnitudes of the excursions of μ' have physical significance.

The principal features of the pattern, Fig. 2(*a*), are (1) the sequence of major peaks, corresponding to excursions of μ' which are largely symmetrical; (2) a series of smaller peaks mainly of an asymmetric nature but symmetrically disposed about $\omega = 90°$; and (3) the contrast between the low plateau around $\omega = 90°$ and the otherwise slightly higher background value of μ' below $\omega = 87$ and above 93°. The observed pattern is symmetrical about $\omega = 90°$ and by implication also about $\omega = 0°$.

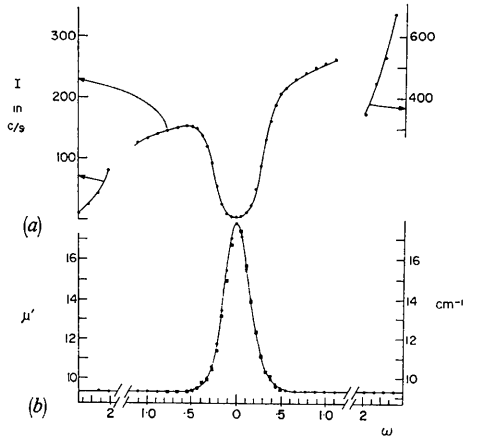

Fig. 1. Measurement of the transmitted beam in the region of the 0002 Bragg reflexion of pyrolytic graphite (Union Carbide, grade ZYA). Measurements were made point-by-point at 0·02° intervals. This corresponds approximately to the region $\omega = 11$–$16°$ in Fig. 2(*a*). (*a*) Displayed as counts/s. (*b*) Converted to μ'.

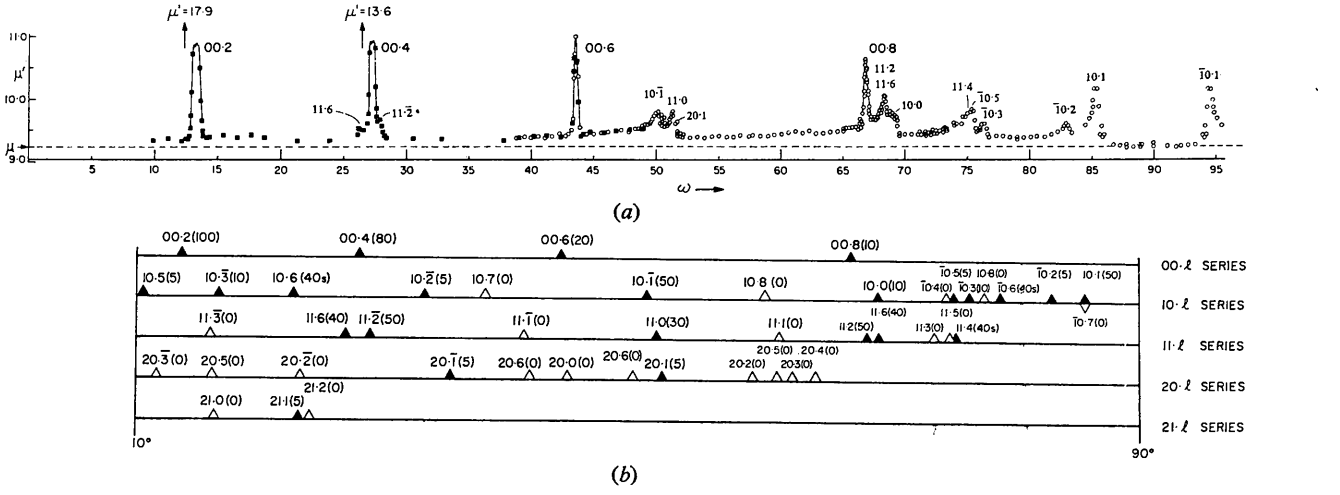

Fig. 2. (*a*) The plot of μ' against ω over the range $\omega = 10$ to 95°. $\omega = 90°$ corresponds to the X-ray beam being normal to the specimen plane [see Fig. 3(*a*)]. (*b*) Key to identification of the TBAP peaks, based on the construction in Fig. 3(*b*). For clarity, the various *hk* series are displayed separately. With each index, the value in brackets corresponds to the diffraction pattern intensity (Cu $K\alpha$) for graphite (JCPDS card 23–64). All interactive indices are recorded; those with nominally zero intensity are identified by open triangles.

Interpretation

For a turbostratic structure such as HOPG with order parallel to the c axis and rotational disorder about that axis, the reciprocal space equivalent, *reseq*,* consists of 000*l* points and *hki*0 and *hkil* rings (Fig. 3*b*).

Because of the range of angular misorientation of the crystallites, the *reseq* distribution is slightly smeared out, being pivoted about the origin; the extent of angular deviation, $\sim\frac{1}{2}°$, is exaggerated in Fig. 3(*b*).

From consideration of the interaction of the *refls* with the *reseq* as ω is altered, the orientations at which diffraction processes are excited and energy is abstracted from the transmitted beam can be correlated with the results presented in Fig. 2.

* It is not appropriate to use the term reciprocal lattice here because of the rotational symmetry. By analogy with Ramachandran & Wooster (1951), the term, *reseq*, reciprocal space equivalent, is introduced instead since it has the appropriate general significance; similarly, *refls* is used for reflecting sphere.

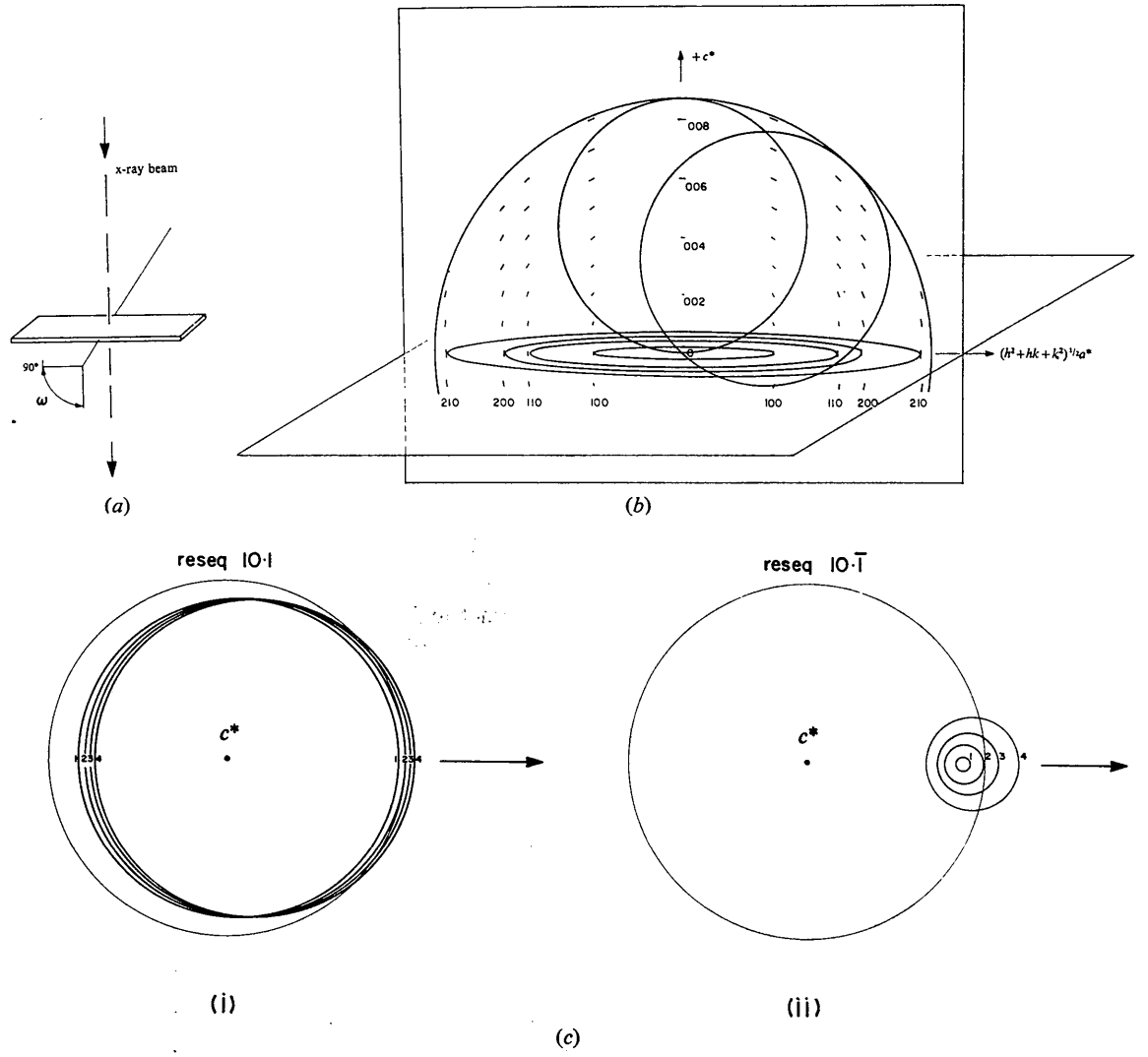

Fig. 3. (*a*) Orientation of the specimen relative to the incident X-ray beam. (*b*) The reciprocal space equivalent, *reseq*, of the pyrolytic graphite specimen is indicated relative to the Ewald sphere, *refls*, for Cu $K\alpha_1$ shown only in vertical section. The smearing of the *reseq* features around the origin point 000 due to the angular divergence of the specimen crystallites is indicated. On this scale, it is exaggerated in order to indicate its shape. Only the *hki*0 *reseq* rings are shown in full (horizontal plane), those for *hkil* being shown simply in the vertical section to prevent visual confusion. With the assumption of anticlockwise movement of the *reseq* relative to the Ewald sphere, intersections on the right-hand side of the origin are arbitrarily identified by a positive h index, on the left by a negative h index. Since the *hkil reseq* is a ring, the sign of the index has no structural significance. Two positions of the *refls* are shown. One corresponds to $\omega = 90°$ [as in (*a*)] while the other corresponds to the value of $\omega \sim 50°$ when the *refls* intersects 10.$\bar{1}$ [see (*c*) (ii)]. To assist in visualization, the horizontal plane and a vertical plane through the origin of reciprocal space are delineated. (*c*) Progress, as ω changes, of the section of the *refls* in the plane of (i) *reseq* 10.1 ($\omega \sim 86°$) and (ii) *reseq* 10.$\bar{1}$ ($\omega \sim 50°$). Four stages (1, 2, 3, 4) are indicated.

Starting with $\omega = 90°$, there is no intersection of the *refls* with any part of the *reseq* but, in the neighbourhood of $\omega = 86°$, the *refls* begins to intersect the 101 ring; next it intersects with 102, at $\omega \simeq 83°$. At a later stage, 0008, 0006, 0004 and 0002 interact.

For the latter 000*l* interactions, the intersections of the *refls* with the respective smeared-out point yield an essentially symmetrical diffraction and hence an absorption (μ') profile similarly symmetrical. However, for the *hkil* reflexions, the situation is more complex. The *refls* passes through a *reseq* ring and this leads first to a rapid rise in diffraction and hence of μ', followed by a relatively slow decrease as the circular section of the *refls* passes through the *reseq* circle [see Fig. 3(*c*) (i)]. Hence the asymmetric shape of the μ' (*hkil*) profiles. Except in the ω region, 87–93°, coincidences of the *refls* and the *reseq* rings produce significant profile tails which cumulatively provide the raised horizon of μ' above the base-line value, μ. Because of the symmetrical disposition of the μ' (*hkil*) profiles about $\omega = 90°$ and the effective non-coincidence of any significant *reseq* ring and the *refls*, this region is free of any interaction.

To assist in the identification of the TBAP peaks, the data for the graphite powder diffraction pattern from the JCPDS file (card 23–64) has been used in preparing the key given in Fig. 2(*b*). For ease of identification, the reflexions are grouped into *hk* series. All reflexions lying within the reflecting circle have been recorded. However, those with intensity effectively zero are identified by unfilled triangles. The indexing, on the basis of the diagram in Fig. 3(*b*), utilized the parameters given in the JCPDS card which may differ slightly from the actual values for the specimen of pyrolytic graphite in use (*vide* Moore, 1973).*

Inspection of Fig. 2 reveals that, although associated with equivalent *reseqs*, the 10.1 peak at $\omega \simeq 86°$ and that of 10.$\bar{1}$ at $\omega \simeq 50°$ differ in shape, noticeably in peak height. The reason for this difference is associated with the magnitude and rate of intersection of the *refls* with the respective *reseq*. For $\omega \simeq 86°$, the section of the *refls* in the plane of the *reseq* 10.1 is compatible with the dimension of the *reseq*, Fig. 3(*c*) (i), so that as ω changes, the interaction rises rapidly and dies off relatively rapidly but, of course, asymmetrically. For $\omega \simeq 50°$, the *refls* is not far from tangential to the plane through *reseq* 10.$\bar{1}$ so that the corresponding section of the *refls* in the plane of *reseq* 10.$\bar{1}$ is much smaller than the dimension of the *reseq*, Fig. 3(*c*) (ii). As a result, even though the section expands rapidly with decrease of ω, the interaction rises and falls far more slowly than for 10.1.

The case of the *reseq* 10.1 and 10.$\bar{1}$ represent the extremes of interaction with the *refls*. Clearly, prediction of the shapes of peaks in the TBAP (and conversely deductions from the shapes) will require precise assessment of the interaction of the *refls* with the *reseq*.

While the experimental set-up involved a σ polarization factor of 1·0 over the full range for diffraction in the horizontal (*i.e.* reflexion) plane, some relaxation of this condition – with intrusion of the π component – would occur for *hkil* reflexions because of the mode of interaction of the *reseq* ring with the *refls*. This relaxation would progressively affect the tails of the asymmetric profiles.

In a recent study of pyrolytic graphite as a monochromator for neutrons, Dorner & Kollmar (1974) gave a brief description of the reciprocal space equivalent (*reseq*) of pyrolytic graphite and its intersection with the Ewald sphere. Their treatment did not extend over the full ω range but was restricted to a small range of rocking angle and was limited to discussion of what they referred to as 'parasitic' reflexions near the main Bragg dip in their transmitted-beam curve (shown as % transmission).

Discussion

The transmitted-beam absorption pattern and the diffraction pattern are complementary but their precise relationship is not immediately obvious. In the case of the diffraction pattern, the individual diffraction events are recorded at their respective values of 2θ as the *reseq* intersects the *refls* but information on the ω sequence is not registered. In the case of the transmitted-beam absorption pattern, ω is the variable and no information concerning 2θ is registered. Since both position and amplitude are relevant in identifying and comparing these two patterns, the complementarity is most evident between the μ' presentation of the transmitted-beam absorption pattern and the diffraction pattern in which the intensity excursions are recorded as log *I*.

While an interpretation of the μ' pattern for pyrolytic graphite has been offered in the previous section, no attempt has been made here to derive any numerical information concerning the significance of the exact shapes and magnitudes of the *hkil* μ' profiles in relation to the corresponding (log) intensities of the diffraction pattern. This correlation would be of obvious interest.

Pyrolytic graphite is a valuable representative of structures of turbostratic type because it is monatomic. However, many clays also belong to this type and should warrant investigation using this technique.

In respect of the TBAP, the case of the turbostratic structure lies between the two extremes of the single crystal and the specimen made of powdered fragments which are oriented in all directions completely randomly. For the single crystal, the *reseq* intersects the *refls* only on the satisfying of very specific conditions, so that the TBAP will consist of a base value of μ with very sharp isolated excursions of μ' from this baseline. By contrast, for the powder sample, the

* According to JCPDS card 23–64, reflexions 10.6 and 11.4 share intensity 40. From the TBAP, Fig. 2, it is clear that the intensity of 10.6 is close to zero; a calculation of the powder-pattern intensities confirmed this conclusion.

spheres of the *reseq* always intersect the *refls* whatever the orientation of the specimen, so that the baseline of the TBAP in this case is not μ but some larger value dependent on the energy abstracted by the simultaneous diffraction of the whole powder pattern.

These observations have relevance to the experimental measurement of attenuation coefficients. Thus, for pyrolytic graphite and Cu $K\alpha_1$ radiation, a region of zero excitation is found to exist near $\omega = 90°$. In fact, a plateau extends from $\omega = 87$ to 93°. It is therefore in this region that a physically valid value of the attenuation coefficient, free of extraneous scattering processes, can be determined experimentally for carbon (Calvert, Killean & Mathieson, 1975). At any value of ω outside this region, contributions from other scattering processes will lead to a value larger than the proper baseline value. These observations stress the recognized (*e.g.* Weiss, 1966; *International Tables for X-ray Crystallography*, 1962) but sometimes overlooked problems associated with the measurement of attenuation coefficients with powdered samples. They also establish the preferential use of either single-crystal material or material of established preferred orientation in the experimental determination of attenuation coefficients.

In measurements on powders, when high accuracy is sought, it is necessary to recognize and estimate preferred orientation in samples so as to allow the application of appropriate corrections. De Wolff & Sas (1969) have dealt with this matter in relation to the diffraction pattern. It would appear from the discussion above that simultaneous determination of the TBAP would be a valuable adjunct in such studies. In general, the transmitted-beam absorption measurement could constitute a valuable indicator of the existence of preferred orientation which might not be simultaneously evident on the part of the diffraction pattern under investigation.

Indeed, the possibility of simultaneous measurement of both transmitted and reflected beams (Calvert, Killean & Mathieson, 1976) would considerably increase insight into the physical processes involved and provide necessary constraints on interpretations based on only one type of observation.*

For measurement of transmitted-beam absorption patterns on material of greater crystalline order than pyrolytic graphite, beams of plane-polarized X-rays of much smaller angular divergence would be advantageous. The possibilities of a synchrotron source in this context (*e.g.* Marr, 1974; Hart, 1975) are evident.

* Thus Urban & Hoseman (1972), restricted to diffraction data assume a constant value of μ' across the reflexion profile. Calvert, Killean & Mathieson (1974*a*), from reflexion and transmission measurements, observe a rapidly varying value of μ' in the Bragg profile (*vide* Fig. 1).

References

BRAGG, W. H. (1914). *Phil. Mag.* 27, 881–899. Reproduced in *Acta Cryst.* (1969). A**25**, 3–11.

CALVERT, L. D., KILLEAN, R. C. G. & MATHIESON, A. MCL. (1974*a*). *Diffraction Studies of Real Atoms and Real Crystals*, pp. 88–89. Canberra: Australian Academy of Science.

CALVERT, L. D., KILLEAN, R. C. G. & MATHIESON, A. MCL. (1974*b*). *J. Appl. Cryst.* **7**, 406.

CALVERT, L. D., KILLEAN, R. C. G. & MATHIESON, A. MCL. (1975). *Acta Cryst.* A**31**, 855–856.

CALVERT, L. D., KILLEAN, R. C. G. & MATHIESON, A. MCL. (1976). To be published.

CHIPMAN, D. R. (1969). *Acta Cryst.* A**25**, 209–213.

DORNER, B. & KOLLMAR, A. (1974). *J. Appl. Cryst.* **7**, 38–41.

HART, M. (1975). *J. Appl. Cryst.* **8**, 436–445.

International Tables for X-ray Crystallography (1962). Vol. III, pp. 57 *et seq.* Birmingham: Kynoch Press.

MARR, S. V. (1974). *Endeavour*, **33**, 55–59.

MATHIESON, A. MCL. (1968). *Rev. Sci. Instrum.* **39**, 1834–1837.

MOORE, A. W. (1973). *Chemistry and Physics of Carbon*, Vol. XI, pp. 69–187. Edited by P. L. WALKER & P. A. THROWER. New York: Marcel Dekker.

RAMACHANDRAN, G. N. & WOOSTER, W. A. (1951). *Acta Cryst.* **4**, 335–344.

URBAN, J. & HOSEMANN, R. (1972). *Acta Cryst.* A**28**, 40–46.

WEISS, R. J. (1966). *X-Ray Determination of Electron Distributions*. Amsterdam: North Holland.

WOLFF, P. M. DE & SAS, W. H. (1969). *Acta Cryst.* A**25**, 206–209.